Longitudinal immune monitoring of patients with resectable esophageal adenocarcinoma treated with Neoadjuvant PD-L1 checkpoint inhibition

Tom van den Ende, Aiarpi Ezdoglian, Lisanne M. Baas, Joyce Bakker, Sinéad M. Lougheed, Micaela Harrasser, Cynthia Waasdorp, Mark I. van Berge Henegouwen, Maarten C.C.M. Hulshof, Nadia Haj Mohammad, Richard van Hillegersberg, Stella Mook, Conny J. van der Laken, Nicole C.T. van Grieken, Sarah Derks, Maarten F. Bijlsma, Hanneke W.M. van Laarhoven & Tanja D. de Gruijl

View supplementary material

Published online: 17 Jul 2023.

Submit your article to this journal

Article views: 411

View related articles

View Crossmark data

Taylor & Francis
Taylor & Francis Group

ORIGINAL RESEARCH

🔓 OPEN ACCESS | Check for updates

Longitudinal immune monitoring of patients with resectable esophageal adenocarcinoma treated with Neoadjuvant PD-L1 checkpoint inhibition

Tom van den Ende [ID][a,b], Aiarpi Ezdoglian[c,d,e], Lisanne M. Baas[c,e], Joyce Bakker[c,e], Sinéad M. Lougheed[c,e], Micaela Harrasser[c,e,f], Cynthia Waasdorp[e,f,g], Mark I. van Berge Henegouwen[h,i], Maarten C.C.M. Hulshof[f,j], Nadia Haj Mohammad[k], Richard van Hillegersberg[l], Stella Mook[m], Conny J. van der Laken[d], Nicole C.T. van Grieken[e,n], Sarah Derks[c,e,f], Maarten F. Bijlsma[e,f,g], Hanneke W.M. van Laarhoven[a,b], and Tanja D. de Gruijl[c,e]

aDepartment of Medical Oncology, Amsterdam UMC, University of Amsterdam, Amsterdam, The Netherlands; bCancer Center Amsterdam, Imaging and Biomarkers, Amsterdam, The Netherlands; cDepartment of Medical Oncology, Amsterdam UMC, Vrije Universiteit Amsterdam, Amsterdam, Netherlands; dAmsterdam UMC, Vrije Universiteit Amsterdam, Department of Rheumatology and Clinical Immunology, Amsterdam Institute for Infection and Immunity, Amsterdam, The Netherlands; eCancer Center Amsterdam, Cancer Biology and Immunology, Amsterdam, The Netherlands; fOncode Institute, Utrecht, The Netherlands; gLaboratory for Experimental Oncology and Radiobiology, Center for Experimental and Molecular Medicine, Amsterdam UMC, University of Amsterdam, Amsterdam, The Netherlands; hDepartment of Surgery, Amsterdam Umc, University of Amsterdam, Amsterdam, The Netherlands; iCancer Treatment and Quality of Life, Cancer Center Amsterdam, Amsterdam, The Netherlands; jDepartment of Radiotherapy, Amsterdam Umc, University of Amsterdam, Amsterdam, The Netherlands; kDepartment of Medical Oncology, UMC Utrecht, Utrecht University, Utrecht, The Netherlands; lDepartment of Surgery, UMC Utrecht, Utrecht University, Utrecht, The Netherlands; mDepartment of Radiotherapy, UMC Utrecht, Utrecht University, Utrecht, The Netherlands; nDepartment of Pathology, Amsterdam UMC, Vrije Universiteit Amsterdam, Amsterdam, The Netherlands

ABSTRACT

The analysis of peripheral blood mononuclear cells (PBMCs) by flow cytometry holds promise as a platform for immune checkpoint inhibition (ICI) biomarker identification. Our aim was to characterize the systemic immune compartment in resectable esophageal adenocarcinoma patients treated with neoadjuvant ICI therapy. In total, 24 patients treated with neoadjuvant chemoradiotherapy (nCRT) and anti-PD-L1 (atezolizumab) from the PERFECT study (NCT03087864) were included and 26 patients from a previously published nCRT cohort. Blood samples were collected at baseline, on-treatment, before and after surgery. Response groups for comparison were defined as pathological complete responders (pCR) or patients with pathological residual disease (non-pCR). Based on multicolor flow cytometry of PBMCs, an immunosuppressive phenotype was observed in the non-pCR group of the PERFECT cohort, characterized by a higher percentage of regulatory T cells (Tregs), intermediate monocytes, and a lower percentage of type-2 conventional dendritic cells. A further increase in activated Tregs was observed in non-pCR patients on-treatment. These findings were not associated with a poor response in the nCRT cohort. At baseline, immunosuppressive cytokines were elevated in the non-pCR group of the PERFECT study. The suppressive subsets correlated at baseline with a Wnt/β-Catenin gene expression signature and on-treatment with epithelial–mesenchymal transition and angiogenesis signatures from tumor biopsies. After surgery monocyte activation (CD40), low CD8+Ki67+ T cell rates, and the enrichment of CD206+ monocytes were related to early recurrence. These findings highlight systemic barriers to effective ICI and the need for optimized treatment regimens.

Introduction

The main treatment modality for locally advanced resectable esophageal adenocarcinoma (rEAC) is a combination of chemotherapy, radiotherapy, and surgery. In several countries the neoadjuvant CROSS regimen is considered a standard of care for rEAC.[1] However, despite the benefit of neoadjuvant chemoradiotherapy (nCRT) over surgery alone, 49% of patients will develop disease recurrence within 5 years.[2] Recently, the CheckMate 577 trial established the value of adjuvant nivolumab (anti-PD-1 antibody) in patients with residual disease

after nCRT.[3] The hazard ratio for disease recurrence or death was 0.69 (95% CI, 0.56 to 0.86) in favor of the nivolumab arm.

In a non-randomized phase II study (PERFECT) we investigated whether the addition of an immune checkpoint inhibitor (ICI), atezolizumab (anti-PD-L1), to nCRT enhanced the efficacy of neoadjuvant treatment.[4] Treatment was feasible but there was no significant difference in response or survival compared to a propensity matched nCRT cohort.[4] However, there is a strong relationship between pathological complete response (pCR) and long-term outcome, not only for

chemoradiation in esophageal cancer but also for neoadjuvant ICI.[5,6] Identifying factors related to pathological response could lead to better patient selection through biomarkers or identify mechanisms of treatment resistance. In several tumor types flow cytometry of peripheral blood mononuclear cells (PBMCs) has identified a number of checkpoint molecules and cell types which are altered under the influence of systemic therapy.[7,8] In patients with lung cancer and melanoma treated with anti-PD-1 or anti-CTLA-4 immunotherapy, complete and partial radiological responders had higher expression of PD-1 on CD8+ on-treatment or more baseline CD69+ natural killer (NK) cells compared to non-responders.[9,10] In poor responders higher frequencies of inhibitory myeloid-derived suppressor cells (MDSCs) or regulatory T cells (Tregs) were found in patients treated with an anti-CTLA-4 antibody (melanoma) or a bi-specific T cell engager (B-precursor acute lymphoblastic leukemia).[11,12] Flow cytometry of immune cells thus provides important clues for response and resistance mechanisms in the immunotherapy setting.

The abundance of certain PBMC subsets in different response groups is most likely driven by inter-compartmental cross-talk between the tumor microenvironment (TME), lymph nodes, and the blood compartment.[8] Local immune evasion harnessed by tumor cells can affect immune cell subsets within the TME and, through the lymph nodes, may have a profound influence on the PBMC compartment.[8,13] A relevant example of the aforementioned crosstalk in the context of esophageal cancer is the release of TGF-β from cancer cells in response to radiation, which can lead to the expansion of immunosuppressive Tregs *in vitro*.[14] The release of therapy-induced TGF-β has also been linked in rEAC to epithelial to mesenchymal transition (EMT).[15] EMT is characterized by the gradual transformation of epithelial cells to a mesenchymal phenotype which endows them with more immunosuppressive and migratory properties.[16,17] However, it is not yet known whether the immunosuppression associated with EMT in the TME can be measured in the peripheral blood. Besides offering novel prognostic or predictive parameters, this may have important implications for the design of new therapeutic strategies based on combined immunotherapeutic approaches. We hypothesize that immunosuppressive pathways such as EMT activated within the TME are reflected in PBMC subsets.

In this immune monitoring study, we aimed to identify differential immune profiles based on response status through 14-color-flow cytometry phenotyping of PBMCs and serum cytokine measurements of ICI + nCRT treated rEAC patients before and throughout treatment. Flow cytometry results were compared with an nCRT cohort to find signatures specific for the neoadjuvant ICI combination. In addition, an exploratory analysis was performed on the relationship between PBMC subsets and transcriptomic signatures measured in tumor biopsies.

Patients and methods

This is a translational exploratory immune profiling substudy of the previously published single-arm PERFECT trial (NCT03087864) investigating the safety and efficacy of atezolizumab, a PD-L1 antibody, combined with nCRT, and subsequent esophagectomy for patients with rEAC.[4] In this trial we collected blood samples including heparin and serum tubes at baseline (B), on-treatment in week 5 (OT), before surgery (S) and 3 months after surgery (FU). From the heparin tubes, PBMCs were isolated by gradient centrifugation for flow cytometry analysis, and serum was stored at −80°C for cytokine measurements. An exploratory comparison of the flow cytometry results was performed with a previously published rEAC cohort treated with nCRT without ICI.[7] Both cohorts included histologically confirmed, stage II and III esophageal- or gastro-esophageal junction adenocarcinomas treated with nCRT given according to CROSS.[1] All patients provided written, informed consent for study participation. This study was conducted in accordance with the Declaration of Helsinki and the international standards of good clinical practice.

Patient groups

A selection of 24 patients from the PERFECT trial were included for this immune monitoring study based on response to neoadjuvant treatment. Response was assessed after neoadjuvant therapy by PET-CT to rule out pre-operative progression and for patients who proceeded to surgery by the pathologist in the resection specimen according to the tumor regression grade (TRG). In this study we included the pathological complete responders (pCR; ypT0N0; $n = 9$) and a representative selection of the non-pCR patients ($n = 15$) with subtotal (ypT0N+ or TRG2; $n = 5$), partial responders (TRG4; $n = 5$) and patients with pre-operative progression ($n = 5$). From the nCRT-only cohort all 26 patients were included as exploratory comparator to the PERFECT study.[7] From the 26 patients, seven had a pCR and 19 had residual disease in the resection specimen (non-pCR).

PBMC isolation

PBMCs were isolated from heparinized blood (20 ml) and cryopreserved until analysis, all as previously described.[18] In brief, a ficoll (Lymphoprep, STEMCELL technologies) gradient centrifugation protocol was used to isolate the PBMC fraction. The PBMC fraction was viable frozen with cell freezing medium (25% dimethyl sulfoxide, 75% fetal calf serum) and stored in liquid nitrogen until defrosted upon analysis.

Flow cytometry of PBMCs

Flow cytometry was performed on thawed PBMCs with multicolor panels to characterize the frequency and activation status of lymphocytic, dendritic, monocyte, and myeloid subsets as previously published.[7] The samples collected before, during, and after treatment were stained according to customized panels (Table S1) and measured on a flow cytometer (LSRFortessa, BD). Due to a remarkably higher activation of monocytes in patients with a poor outcome at FU, the samples were further characterized by a panel based on different macrophage markers (Table S2). Patients were stained in multiple batches in a random order to make sure the response groups were not acquired together. Standard compensations for every channel were made and updated to ensure consistency in the obtained results. Application settings were used to ensure the reproducibility of the experiments. Non-lineage markers were gated against

a control tube without the fluorophores of interest. For gating procedures in FCS Express Version 6, see Fig. S1-S3.

Serum cytokine measurements

Thawed serum samples were only available and used from the PERFECT trial at baseline, on-treatment, and before surgery. Serum samples were tested by enzyme-linked immunoassay (ELISA; R&D Systems, DuoSet, Minneapolis, Minnesota) to measure latent and active TGF-β1 according to the instructions of the manufacturer. A custom cytokine panel (IL-6, IL-8, IL10, CXCL9, CXCL10, CCL2, CCL5, and VEGF) was used to measure serum levels by cytometric bead array (CBA; BD, Flex-set, Franklin Lakes, New Jersey) on the LSRFortessa according to manufacturer's instructions. Measurement of supernatant through CBA (IL-6, IL-8, IL10, CXCL10, TNF, CCL2, and CCL5) from magnetic-activated cell sorted CD14+ PBMCs from the FU time-point was done before and 24 h after stimulation according to the following conditions: M1 (100 ng/ml LPS and 20 ng/ml IFN-γ) M2a (10 ng/ml IL-4 and 10 ng/ml IL-10) and Poly IC (100 ug/ml).

RNA-sequencing data-set

The previously reported RNA-sequencing set with baseline and on-treatment biopsies from PERFECT (GSE165252) was used to correlate PBMC subsets to the MSigDB Hallmark gene sets.[19] Moreover, exploratory sub-analyses were performed based on a library of EMT signatures (EMTome) and a canonical 16-gene EMT signature validated in a pan-cancer cohort of The Cancer Genome Atlas (TCGA).[20,21] This 16-gene EMT signature consists of 13 mesenchymal markers (VIM, CDH2, FOXC2, SNAI1, SNAI2, TWIST1, FN1, ITGB6, MMP2, MMP3, MMP9, SOX10, GCS) and three epithelial marker genes (CDH1, DSP, and OCLN).[21] An EMT score per biopsy was calculated by adding up the values of the log2 transformed values for the mesenchymal markers subtracted by the epithelial markers. Changes between baseline and on-treatment were calculated by the following calculation: delta EMT = on-treatment EMT score minus baseline EMT score. A validated three-gene signature (CCR8, MAGEH1, and LAYN) was used to estimate the abundance of intratumoral Tregs by calculating a Z-score across biopsies, and this was correlated with the MSigDB Hallmark gene sets.[22]

Statistical analyses

The unpaired T-test (normal distribution) was used to compare the pCR to the non-pCR group for each immune cell subtype and the expression of surface proteins within subsets. For the FU samples from PERFECT we compared patients with a recurrence vs. no recurrence with the unpaired T-test (normal distribution). The Mann – Whitney U test was used to compare changes between time-points and the cytokine levels between the pCR and non-pCR groups as this data was not normally distributed. Longitudinal analyses were tested through a mixed-effects model to assess the overall change over time. Correlations were assessed through the Pearson correlation coefficient. The Cox proportional-hazards model including the logrank test was used to compare progression-free survival (PFS) and disease-free survival (DFS). The application Cutoff Finder or split on the median was used to stratify patients in two groups for Kaplan – Meier analysis.[23] Data cutoff for the survival analyses was 04-01-2021. GraphPad Prism version 9.1 and SPSS version 26.0 (IBM) were used for statistical analyses. An α below 0.05 was regarded as statistically significant. All statistical tests were conducted two-sided.

Results

The baseline characteristics and clinical outcomes of included PERFECT trial patients ($n = 24$) are described in Table 1. Clinical characteristics from the nCRT-only cohort are also given in Table 1 and were comparable to those of PERFECT patients.[7] Baseline and on-treatment samples were available in PERFECT from 24 patients, before surgery from 16 and 3 months after surgery from 15 patients. In the nCRT-only cohort baseline samples were available from 26 patients, on-treatment from six patients and before surgery from 13 patients.

Immunosuppressive PBMC profiles observed in non-complete responders

Multicolor flow cytometry was performed on PBMCs of rEAC patients to assess systemic immune changes before and throughout treatment, Figure 1a. At baseline we observed distinct differences in the main immune cell subsets between the response groups of the PERFECT trial (pCR vs. non-pCR) as shown in a heatmap, Figure 1b. A higher mean % of immunosuppressive Tregs (3.48% vs. 4.60%, $p = 0.02$; Figure 1c) was found in the non-pCR group, while the pCR group had a higher % of type-2 conventional dendritic cells (cDC2; 0.45% vs. 0.27%, $p = 0.003$; Figure 1d). Two suppressive subsets from the myeloid lineage were also more abundant in the non-pCR group: intermediate monocytes (IM; CD14+CD16+, 1.94% vs. 3.68%, $p = 0.01$; Figure 1e) and early myeloid-derived suppressor cells (eMDSCs; lineage-CD14-HLA-DR-CD33+CD11b+, 0.24% vs. 0.61%, $p = 0.04$; Figure 1f). Next, we assessed different immune stimulatory and suppressive checkpoints on each subset. Only CTLA-4+ expression on CD8+ T cells (pCR 2.75% vs. non-pCR 5.36%, $p = 0.01$; Figure 1g) and HLA-DR+ on CD16-CD56+ NK cells (pCR 52.80% vs. non-pCR 36.95%, $p = 0.03$; Figure 1h) differed significantly between both response groups at baseline. Additionally, we investigated if baseline PBMC subsets were related to survival: a high percentage of Tregs (Log-rank $p = 0.04$) and low number of cDC2 (Log-rank $p = 0.03$) were both associated with poor PFS while IM and eMDSCs were not, Fig. S4.

In the PERFECT trial we evaluated the dynamics of the following major PBMC subtypes: T cells (CD3), monocytes (CD14), B cells (CD19), and NK cells (CD56) by a mixed-effects model. A significant drop in T cells was observed irrespective of response on-treatment (Figure 2a). This was accompanied by an increase in the monocyte fraction (Figure 2b). Moreover, on-treatment the % of B cells

Table 1. Baseline characteristics and clinical outcomes from both patient cohorts.

Variables	PERFECT ($n = 24$)	nCRT-only ($n = 26$)
Age, years		
Median	66	67,5
Range	(40-73)	(42-79)
Sex		
Male	21 (87.5)	21 (80.8)
Female	3 (12.5)	5 (19.2)
Clinical tumor stage		
cTx	0	1 (3.8)
cT2	6 (25)	2 (7.7)
cT3	17 (70.8)	23 (88.5)
cT4a	1 (4.2)	0
Clinical nodal stage		
cNx	0	1 (3.8)
cN0	8 (33.3)	11 (42.3)
cN1	11 (45.8)	10 (38.5)
cN2	5 (20.8)	2 (7.7)
cN3	0	2 (7.7)
Tumor location		
Mid	2 (8.3)	0
Distal	17 (70.8)	21 (80.8)
GEJ	5 (20.8)	5 (19.2)
Pathological response		
pCR	9 (37.5)	7 (26.9)
ypT+ or ypN+ or progression	15 (62.5)	19 (73.1)
Recurrence		
Yes	15 (62.5)	12 (46.2)
No	9 (37.5)	14 (53.8)

Abbreviations: GEJ = gastroesophageal junction; nCRT = neoadjuvant chemoradiotherapy; pCR = pathological complete response.

(Figure 2c) and NK cells (Figure 2d) significantly dropped and recovered in both response groups before surgery. These findings are consistent with myelosuppression due to the co-administration of chemotherapy in the PERFECT trial regimen. Next, we assessed if subsets and checkpoints differed between response groups based on the on-treatment time-point, Figure 2e. A higher percentage of total Tregs (4.13% vs. 6.15%, $p = 0.03$) and activated Tregs (aTregs; CD45RA-FOXP3++, 2.44% vs. 4.25%, $p = 0.003$; Figure 2f) was found in the non-pCR group. In matched baseline and on-treatment samples, the aTreg fraction significantly increased in the non-pCR group, $p = 0.02$; Figure 2g. Interestingly, when we combined a metric for T cell proliferation (CD8+Ki67+) and the aTreg percentage into a ratio, we discovered that the pCR group had a higher ratio compared to the non-pCR group (5.66 vs. 2.79, $p = 0.02$; Figure 2h), indicating less immune suppression in the pCR group. Findings regarding the three different monocyte subsets were comparable to baseline with a higher percentage of CD14+CD16+/CD16++ (respectively intermediate and non-classical) monocytes in the non-pCR group (Figure 2e-i). Moreover, CD14+CD16- classical monocytes were consequentially higher in pCR patients ($p = 0.01$; Figure 2j). Other significant findings on-treatment were a higher CD16+CD56+NK cell fraction ($p = 0.049$; Table S3) and a higher percentage of CD86+ B cells in the pCR group ($p = 0.04$; Table S3). Correlations between subsets and survival revealed a low CD8Ki67/aTreg ratio on-treatment was associated with poor PFS (Log-rank $p = 0.008$), while the aTreg delta or non-classical monocytes on-treatment were not associated with long-term outcome, Fig. S4.

At the before-surgery time-point, the distribution of subsets was again showing higher percentages of CD14+CD16+/CD16++ monocytes but also CD4+CD45RA-CD27+ central memory cells in the non-pCR group. The higher percentage of central memory CD4 T cells after neoadjuvant treatment in non-pCR patients could be related to weak (co-)stimulation of naïve CD4 T cells and their consequent inability to switch to an effector phenotype.[26,27] For the main PBMC subsets we also investigated if changes between baseline and on-treatment or before surgery were associated with pathological response. Besides the change in aTregs, between baseline and on-treatment, there were no other statistically significant differences between response groups, Table S4. A full overview of flow cytometry results from PERFECT can be found in Table S3. In summary based on flow cytometry immune profiling of PBMCs, we observed a higher abundance of immunosuppressive subsets in non-pCR patients.

We next questioned whether our findings were specific for the anti-PD-L1 regimen combined with nCRT in the PERFECT trial. Therefore, we compared our data with results from 26 rEAC patients treated with nCRT-only without ICI from a previously published immune monitoring study.[7] In the nCRT-only cohort we assessed if there was also a difference at baseline in PBMC subsets between response groups, Fig. S5A. Only the percentage of CD8 T-cells was significantly higher in the pCR group (37.54% vs. 21.81%, $p = 0.004$; Fig. S5B). No significant difference was found between the response groups based on the baseline immunosuppressive subsets (Tregs, CD14+CD16+ IM monocytes, eMDSCs) earlier identified in the PERFECT
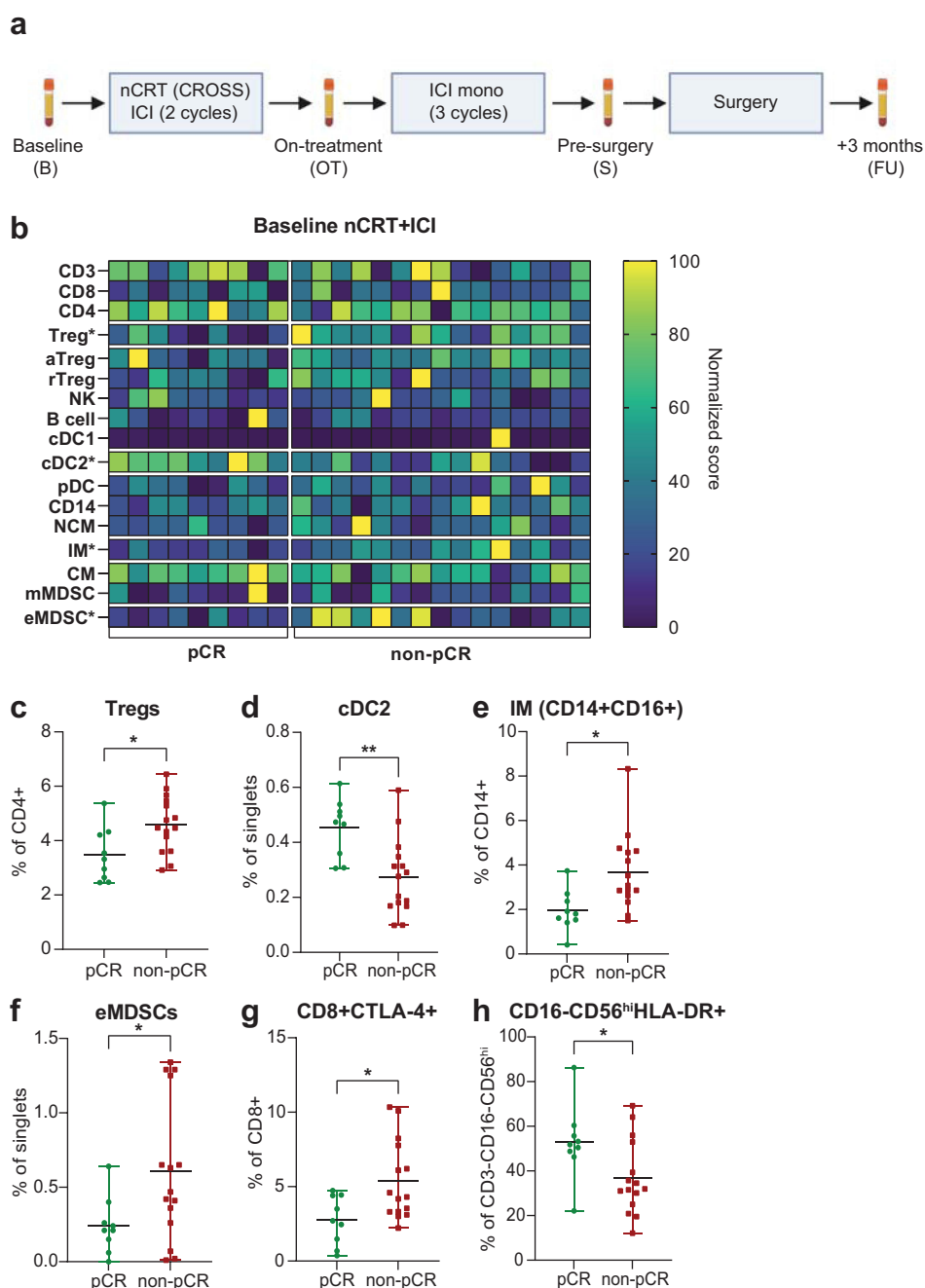
Figure 1. Baseline flow cytometry results of PBMC subsets in patients from the PERFECT trial. a) Treatment regimen with blood sampling schedule from patients treated with anti-PD-L1 combined with neoadjuvant chemoradiotherapy. b) Heatmap of baseline PBMC subset frequencies divided by pCR and non-pCR. The response to neoadjuvant therapy is given on the horizontal axis. Values were normalized between 0 and 100 within each subset based on percentages from singlets (CD3, NK, B cells, cDC1, cDC2, pDC, CD14, mMDSC, eMDSC), parent CD3 (CD8, CD4), parent CD4 (Treg, aTreg, and rTreg) and parent CD14+ (NCM, IM, and CM). The asterisk behind subsets denotes significant differences between the pCR and non-pCR groups. c-h) Baseline PBMC subset and marker frequencies with significant differences between the pCR and non-pCR groups. The pCR and non-pCR groups were statistically tested with the unpaired t-test. Abbreviations: cDC = conventional dendritic cells; CM = classical monocytes; eMDSC = early myeloid-derived suppressor cells; ICI = immune checkpoint inhibitor; IM = intermediate monocytes; mMDSC = mature myeloid-derived suppressor cells; NCM = non-classical monocytes; nCR = non-complete response; nCRT = neoadjuvant chemoradiotherapy; NK = natural killer cell; pCR = pathological complete response; pDC = plasmacytoid dendritic cells; Tregs = regulatory T cells.

trial, Fig. S5C-E. Next, we assessed the dynamics in major subsets which roughly resembled the changes seen in the PERFECT trial with a decrease in T cells and an increase in monocytes, Fig. S6A-B. This was accompanied by a decrease in the % of B cells and a relatively stable % of NK cells, Fig. S6C-D. For the on-treatment time-point, the aTregs, CD8+Ki67+/aTreg ratio, aTregs delta, and non-

classical CD14+CD16++ monocyte graphs are given in the supplementary for illustrative purposes, Fig. S6E-F. Relatively few samples ($n = 6$) were available for the on-treatment time-point in the nCRT-only cohort, and therefore no formal statistics were performed. A full overview of flow cytometry results from the nCRT-only cohort can be found in Table S5. These findings suggest that baseline
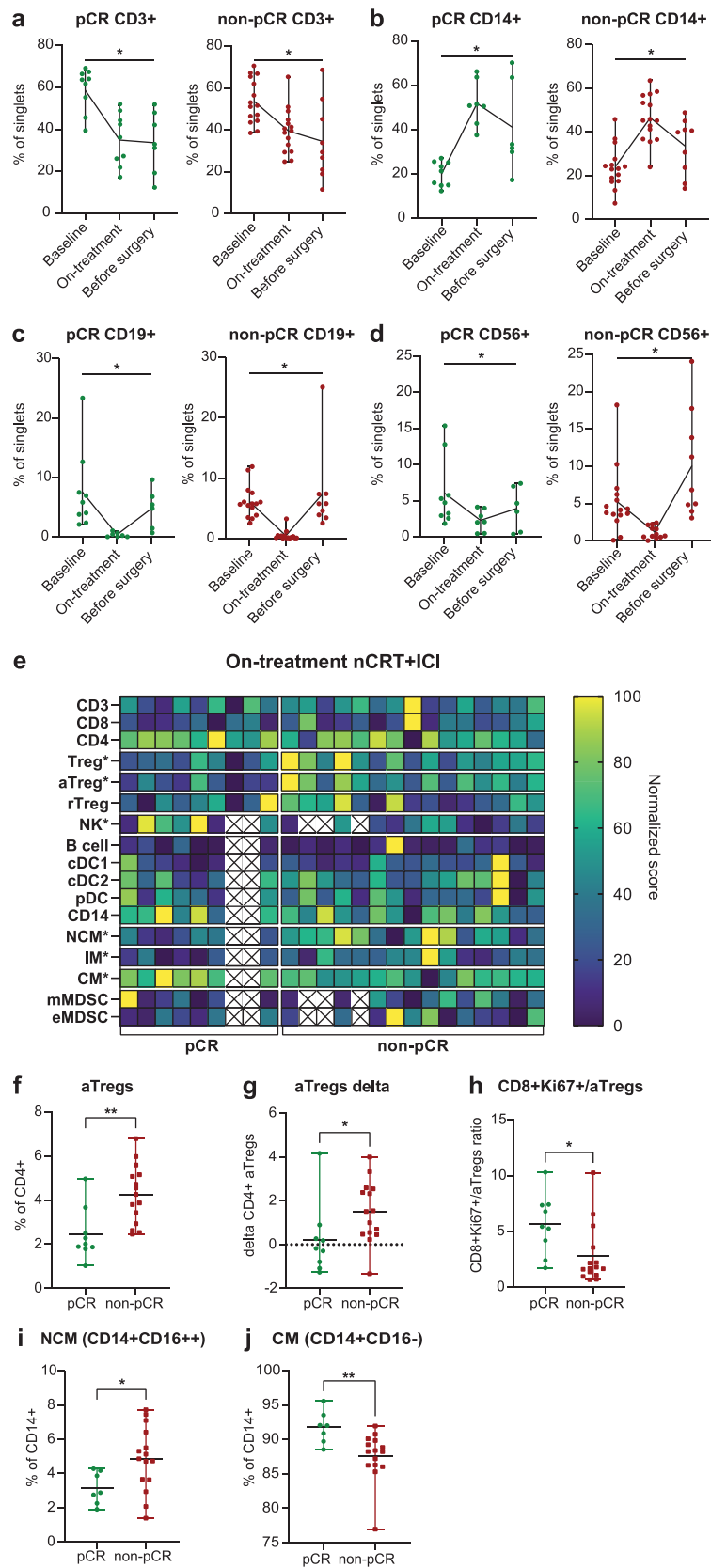
Figure 2. Longitudinal flow cytometry results of PBMC subset rates and marker expression in patients from the PERFECT trial. a) Longitudinal results of CD3+ T cells in the pCR group (green) and the non-pCR group (red). b) Longitudinal results of CD14+ monocytes in the pCR group (green) and the non-pCR group (red). c) Longitudinal results of CD19+ B cells in the pCR group (green) and the non-pCR group (red). d) Longitudinal results of CD56 natural killer cells in the pCR group (green) and the non-pCR group (red). e) Heatmap of on-treatment PBMC subset rates between the pCR and non-pCR groups. Data were normalized within each subset. For some patients no data were available from specific markers due to insufficient cells for flow cytometry analysis. This is marked by an empty box with a cross. Values were normalized between 0 and 100 within each subset based on percentages from singlets (CD3, NK, B cells, cDC1, cDC2, pDC, CD14, mMDSC, eMDSC), parent CD3 (CD8, CD4), parent CD4 (Treg, aTreg, and rTreg) and parent CD14+ (NCM, IM, and CM). The asterisk behind subsets denotes significant differences between the pCR and non-pCR groups. f) Activated Treg frequencies on-treatment with the individual values for the pCR and non-pCR groups. The pCR and non-pCR groups were statistically tested with the

Table 2. Main baseline flow cytometry findings compared between response groups in both cohorts.

Immune subset/marker	pCR nCRT+ICI	non-pCR nCRT+ICI	pCR nCRT-only	non-pCR nCRT-only
Baseline				
CD8+ (of CD3)	25.79 (14.16–37.38)	30.14 (15.19–57.41)	37.54 (15.48–60.3)*	21.81 (8.93–45.6)*
Tregs (of CD4)	3.48 (2.46–5.37)*	4.60 (2.92–6.44)*	3.91 (0.96–9.91)	2.67 (0.43–14.06)
cDC2 (of singlets)	0.45 (0.31–0.61)*	0.27 (0.10–0.59)*	0.73 (0.11–1.75)	1.04 (0.07–2.96)
IM (of CD14)	1.94 (0.41–3.74)*	3.68 (1.50–8.33)*	2.26 (0.1–6.12)	3.79 (0.29–7.26)
eMDSCs (of singlets)	0.24 (0–0.64)*	0.61 (0.01–1.34)*	0.07 (0–0.23)	0.13 (0–0.9)

Mean and range are given for each group. An asterisk denotes statistical significance between both response groups (T-test). Abbreviations: cDC2 = type-2 conventional dendritic cells; eMDSCs = early myeloid derived suppressor cells; ICI = immune checkpoint inhibitor; IM = intermediate monocytes; nCRT = neoadjuvant chemoradiotherapy; pCR = pathological complete response; Tregs = regulatory T cells.

circulating immunosuppressive subsets are associated with therapy resistance in the PERFECT trial but not in patients treated with nCRT-only, Table 2.

Immunosuppressive cytokines elevated in serum of poor responders

We measured several cytokines (TGF-β1, IL-6, IL-8, IL10, CXCL9, CXCL10, CCL2, CCL5, and VEGF) in the serum of patients to assess their relationship to the identified PBMC subsets (observed by cytometry to be related to response) and directly to response to treatment in the PERFECT trial at three time-points: baseline, on-treatment and before surgery. Correlations were assessed between baseline cytokines, Tregs, cDC2, intermediate monocytes, and eMDSCs, Figure 3a. Only activated TGF- β1 positively correlated with the PBMC Treg percentage, $r = 0.58$, $p < 0.01$; Figure 3b. No correlation was found between monocytes and cytokines in serum related to monocyte functionality and recruitment, i.e. CCL2, CCL5, VEGF, TGF-β1, and IL10. This indicates that monocytes are not the sole producers or interactors with these molecules. Comparing correlations between the aforementioned baseline subsets, Tregs were negatively correlated with cDC2 abundance, $r = -0.47$, $p = 0.02$, Figure 3a. On-treatment there was no significant correlation between PBMC subsets such as (a) Tregs or monocytes and cytokine serum levels, Fig. S7.

To assess if there was also a difference in serum markers between response groups in the PERFECT trial, we compared serum levels between pCR and non-pCR patients. At baseline several cytokines showed higher levels in the non-pCR group compared to the pCR group (IL-6 $p = 0.03$, IL-8 $p = 0.02$, IL-10 $p = 0.03$ and VEGF $p = 0.08$; Figure 3c-f). Interestingly, baseline IL-6, IL-10, and VEGF serum levels also correlated with each other, suggestive of a coordinated immune suppressive program in the non-pCR group, Figure 3a, Table S6. The same trend between cytokine levels and non-pCR was observed on-treatment although the difference was not statistically significant (IL-6 $p = 0.10$, IL8 $p = 0.07$, VEGF $p = 0.08$; Fig. S8). At surgery IL-8 ($p = 0.03$), CCL5 ($p = 0.04$) and VEGF ($p = 0.02$) were significantly higher in the non-pCR group, Fig. S8.

Immunosuppressive pathways correlate with circulating PBMC subsets

From the PERFECT trial patients RNA-sequencing data was available from baseline and on-treatment tumor biopsies. The sequencing data was used to identify pathways correlating with the abundance of the identified PBMC subsets differentially present between pCR and non-pCR patients. Baseline percentage of Tregs, cDC2, intermediate monocytes, and eMDSCs were correlated with the MSigDB Hallmark gene sets of matched baseline biopsies ($n = 20$). The Wnt/β-Catenin signaling pathway positively correlated with both Tregs and intermediate monocytes, $p < 0.05$, Figure 4a. Additionally, cDC2 negatively correlated with the pancreas beta cell pathway and intermediate monocytes positively correlated with hedgehog signaling and myogenesis, $p < 0.05$, Figure 4a. The eMDSC percentage correlated with the estrogen response and P53 pathway, $p < 0.05$, Figure 4a. These pathways have all been linked to the expansion of immunosuppressive immune cells or intratumoral immunosuppression.[28–32] A full overview of the baseline correlations can be found in Table S7.

Next, we correlated the circulating aTreg percentage, as the most significant finding on-treatment, to the Hallmark gene sets of matched on-treatment biopsies ($n = 19$). The top three pathways positively correlating with aTregs were angiogenesis, hedgehog, and TGFβ signaling, Figure 4b. We subsequently investigated if intratumoral Tregs were also associated with the same pathways as circulating aTregs. An intratumoral Treg signature (CCR8, MAGEH1, and LAYN) positively correlated in on-treatment biopsies ($n = 31$) with the following top three pathways: UV response down, EMT, and angiogenesis, Figure 4c. Thus, the angiogenesis pathway was positively correlated with both circulating aTregs and intratumoral Tregs. Also, TGF-β signaling and EMT, which were previously found to be related to each other, were at the top of positively correlating pathways, Figure 4b-c, Table S8.[15] Further characterization of the EMT phenotype was done by correlating a library of EMT signatures across tumor types (EMTome) to the circulating aTregs.[20,21] Several EMT signatures positively correlated with circulating aTregs, Table S9. From these signatures we identified a 16-gene pan-cancer EMT signature

unpaired t-test. g) Changes (delta) between baseline and on-treatment rates of activated Tregs with the individual values for pCR and non-pCR groups. The pCR and non-pCR groups were statistically compared with the Mann–Whitney U test. h) The proliferating (Ki67+) CD8 T-cell to activated Treg ratio between the pCR and non-pCR groups on-treatment. The pCR and non-pCR groups were statistically tested with the unpaired t-test. i-j) The CD14+CD16++ non-classical monocytes and CD14+CD16-classical monocytes on-treatment with the individual values for the pCR and non-pCR groups. The pCR and non-pCR groups were statistically tested with the unpaired t-test. Abbreviations: CM = classical monocytes; ICI = immune checkpoint inhibitor; IM = intermediate monocytes; NCM = non-classical monocytes; non-pCR = non-complete response; nCRT = neoadjuvant chemoradiotherapy; pCR = pathological complete response; Tregs = regulatory T cells.
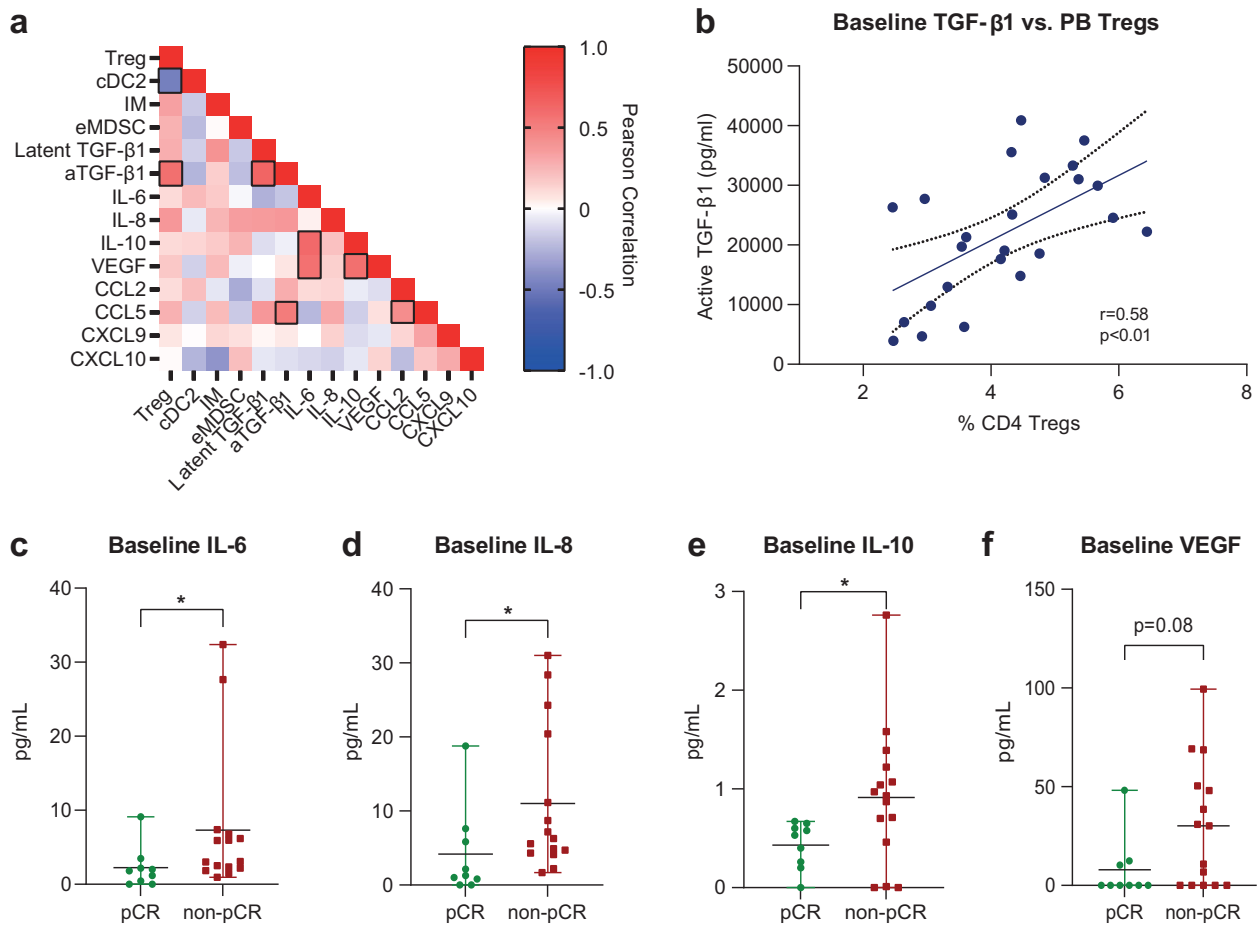
Figure 3. Cytokine levels in serum samples from patients treated in the PERFECT trial. a) Pearson correlation matrix between baseline subset rates and serum cytokine levels. Statistically significant correlations are highlighted by black outlined squares, $p < 0.05$. b) Pearson correlation of CD4+ Tregs and activated TGF-β1 at baseline. c-f) Serum concentrations of IL-6, IL-8, IL-10, and VEGF at the baseline of the pCR and non-pCR groups. The pCR and non-pCR groups were statistically compared with the Mann–Whitney U test. Abbreviations: eMDSC = early myeloid-derived suppressor cells; IL = interleukin; IM = intermediate monocytes; non-pCR = non-complete response; PB = peripheral blood; pCR = pathological complete response; TGF-β1 = transforming growth factor β1; Tregs = regulatory T cells.

previously validated in the TCGA dataset including in EAC samples (see methods). This signature was used to estimate the change in EMT between matched baseline and on-treatment biopsies ($n = 15$). There was a positive correlation between induction of EMT and the change in circulating aTregs, $r = 0.54$, $p = 0.04$; Figure 4d. Interestingly, the CD8Ki67/aTreg ratio negatively correlated with the EMT signature, and based on both markers, two subgroups could be demarcated (gray lines: immunosuppressive low top-left corner vs. immunosuppressive high), $r = -0.56$, $p = 0.01$; Figure 4e. Having established that EMT and the CD8Ki67/aTreg ratio were related to each other, we investigated if both were related to PFS. After combining the on-treatment CD8+Ki67+/aTreg ratio and EMT signature, a relationship with long-term outcome was observed. Patients who were immunosuppressive low (CD8Ki67/aTreg ratio >median 2.31 and EMT low ≤median 91.1) had better PFS compared to immunosuppressive high (CD8Ki67/aTreg ratio ≤median 2.31 or EMT high >median 91.1), HR = 0.32 95% CI 0.12–0.88, $p = 0.04$; Figure 4f. The combined analysis performed better than EMT alone (cutoff

median 91.1, log-rank $p = 0.57$) but not better than the CD8Ki67/aTreg ratio alone (cutoff median 2.31, log-rank $p = 0.02$). These findings suggest that immunosuppressive pathways such as EMT in the TME are related to intratumoral and circulating (a) Tregs and together with the CD8Ki67/aTreg ratio correlates with PFS.

PBMC subsets related to recurrence after surgery

For the 3-month time-point after surgery, we investigated if PBMC subsets or related markers were associated with recurrence of disease in the PERFECT trial. Out of 15 patients with data available from flow cytometry 11 experienced a recurrence vs. four who remained disease-free after a median of 809 days of follow-up. The % of CD8Ki67 positive T-cells was higher in patients without recurrence ($p = 0.04$; Figure 5a). In contrast, the % of intermediate monocytes was higher in patients who developed a recurrence ($p = 0.04$; Figure 5b). Moreover, the % of CD40+ monocytes in all three subsets was related to recurrence (Figure 5c-e). A full overview of flow cytometry results of
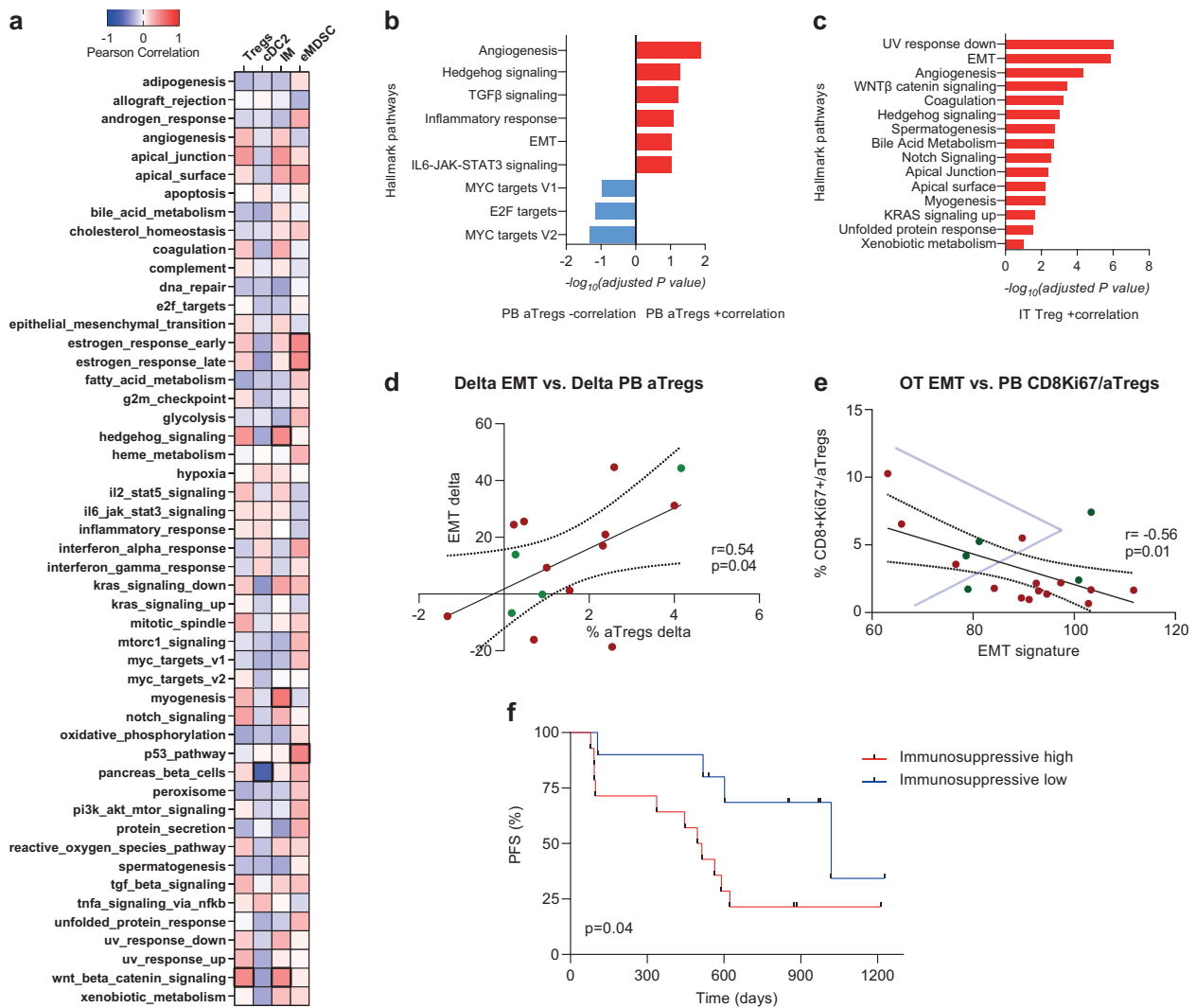
Figure 4. Relationship between transcriptomic signatures in tumor biopsies and PBMC subsets in the PERFECT trial. a) Correlation between the MSigDB Hallmark gene-sets from baseline tumor biopsies and baseline PBMC subsets. Statistically significant correlations are highlighted by black outlined squares, p < 0.05. b) Correlation between the MSigDB Hallmark gene-sets from on-treatment biopsies and on-treatment circulating aTregs which reached a *p* value < 0.1. c) Correlation between the MSigDB Hallmark gene-sets from on-treatment biopsies and on-treatment intratumoral Tregs which reached a *p* value < 0.1. d) Correlation between the delta EMT signature between baseline and on-treatment and the delta aTregs measured by flow cytometry of PBMCs. e) Correlation between an EMT signature and the CD8+Ki67 +/aTreg ratio measured by flow cytometry of PBMCs on-treatment. The gray lines demarcate the immunosuppressive low (top left corner) and immunosuppressive high groups from each other. f) Kaplan-Meier of PFS between patients with who were immunosuppressive low (CD8Ki67/aTreg ratio >median and EMT low ≤median) compared to immunosuppressive high (CD8Ki67/aTreg ratio ≤median or EMT high >median). In case no biopsy was available to measure EMT (n = 5) the CD8+Ki67 +/aTreg ratio was used to classify patients. Abbreviations: aTreg = activated regulatory T cell; EMT = epithelial – mesenchymal transition; OT = on-treatment; PB = peripheral blood; PFS = progression-free survival; Tregs = regulatory T cells.

the follow-up time-point can be found in Table S10. The activation status (CD40 expression) of classical (HR = 0.26 95% CI 0.08–0.88, p = 0.02; Figure 5f) and intermediate monocytes (HR = 0.31 95% CI 0.09–1.01, p = 0.06; Figure 5g) was related to DFS. Patients with low (<median) levels of expression showed superior DFS. To further explore the phenotype of monocytes after surgery based on recurrence status, we developed a flow cytometry panel based on M1 and M2 macrophage markers, Table S2. Only CD206 showed a statistically significant difference between both groups with a higher % of CD14 +CD206+ M2-like monocytes in patients with a recurrence, Figure 5h. In the CD14+CD206+ population a higher % of CD163, CD169, PD-L1, and CD80 expression was found compared to the CD14+CD206- group, Figure 5i. These findings suggest that PBMC from patients with a recurrence are enriched for monocytes with an M2-like suppressive

phenotype 3 months after nCRT/ICI treatment and surgery. Functional stimulation of CD14+ isolated monocytes from PBMCs with LPS/IFNγ (M1-skewing cocktail), IL-4/IL-10 (M2a-skewing cocktail) or poly IC did not reveal any difference in cytokine profile based on recurrence status, Fig. S9.

Discussion

In this immune monitoring sub-study of the anti-PD-L1/nCRT PERFECT trial, we investigated circulating immune cells through flow cytometry analysis and cytokine measurements in patients with rEAC. The non-pCR group had higher percentages of immunosuppressive immune cells and elevated cytokine levels compared to patients who had a pCR. Notably, circulating Treg and monocyte subsets were more abundant, while cDC2 cells were lower in the non-pCR
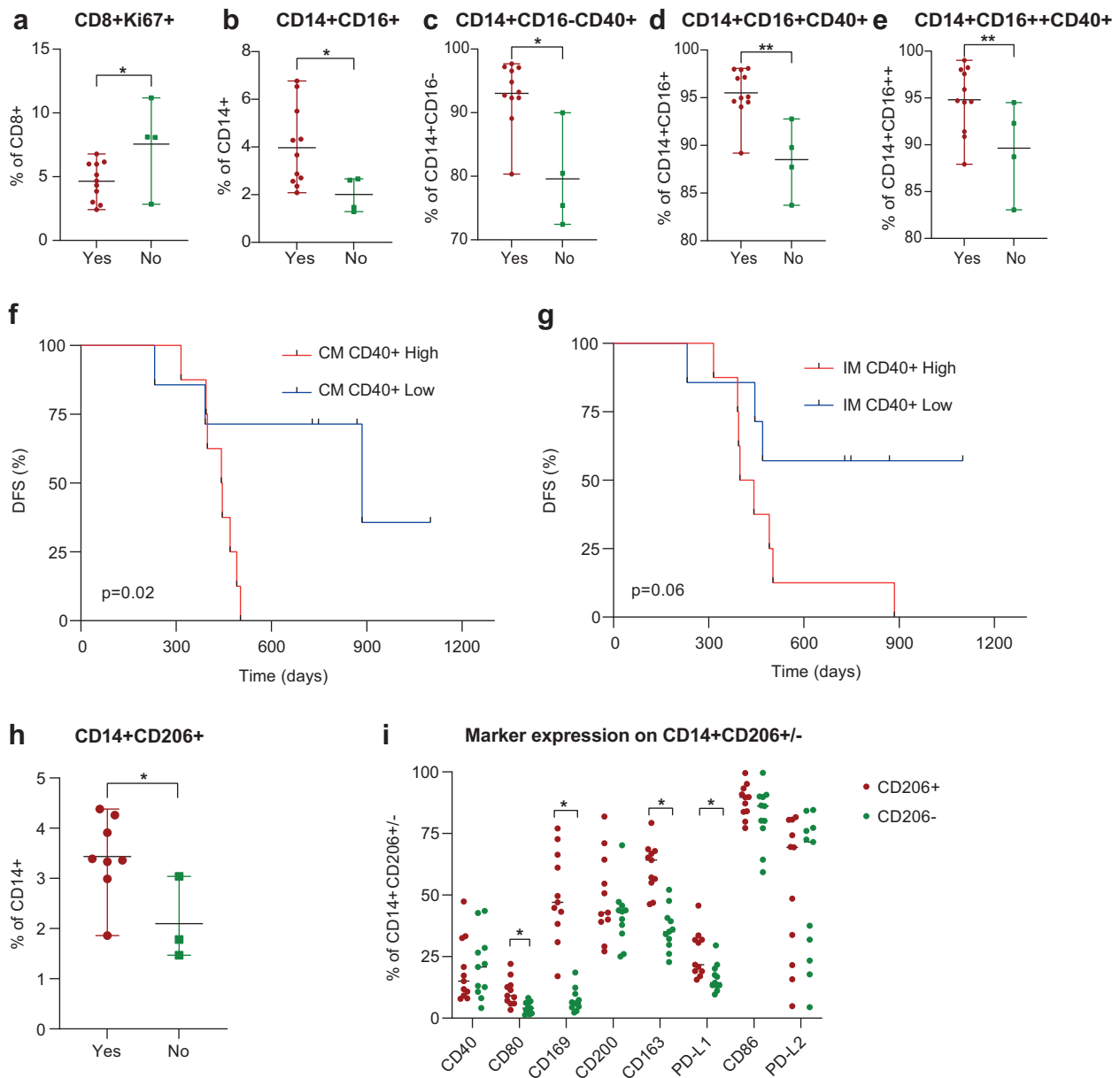
Figure 5. PBMC flow cytometry results three-months after surgery from the PERFECT trial stratified according to eventual recurrence status. a-e) Subset rates and marker expression levels from patients with and without a recurrence (unpaired t-test). Asterisk indicates statistical significance. f-g) Kaplan Maier of DFS between patients who were high or low in their percentage of classical or intermediate monocytes with CD40 expression, based on the median (<median vs. ≥median). h) The percentage of CD14+CD206+ cells in patients with and without a recurrence at FU. i) Macrophage markers across the CD206+ fraction and CD206- fraction from FU PBMC samples. Abbreviations: CM= classical monocytes; FU= three-months after surgery; IM= intermediate monocytes.

group. Interestingly, this was not observed in a cohort of nCRT-only treated patients. Several immunosuppressive pathways in tumor biopsies were positively correlated with circulating Tregs and monocytes. Three months after surgery monocyte activation status, related to an M2-like phenotype, and a lack of CD8+Ki67+ T cells was predictive of recurrence.

By flow cytometry and serum analyses, we observed an immunosuppressive subset profile in non-pCR patients. The non-responders from the PERFECT trial had more Tregs at baseline and an expansion of aTregs on-treatment reflected by a greater increase in the non-pCR group versus the pCR group. Tregs and a ratio for effector/regulatory T-cells have previously been linked to poor response and prognosis in several tumor types.[18,33–35] Moreover, Tregs have been associated with inhibition of cDC2 cells present in tumor draining lymph nodes.[36] The cDC2 cells are in this way not able to support a conventional CD4 T-cell response to anti-PD-1 therapy.[36] In our study we also observed a higher percentage of baseline cDC2 in responders with a relatively lower Treg population. This response pathway related to cDC2 and CD4 anti-tumor immunity might also play a crucial role in rEAC patients treated with anti-PD-L1/nCRT and could be measurable in peripheral blood. Other PBMC subsets related to response were from the myeloid lineage the CD16+ monocytes and eMDSCs which showed higher circulating percentages in the non-pCR group. The presence and expansion of CD16-positive

monocytes has previously been established in several tumor types and is an instrumental subset in the crosstalk between tumor and immune-system, resulting in tumor progression and immune suppression.[37–40] In a recently published article, the intermediate blood monocytes of ovarian cancer patients were related to soluble immunosuppressive mediators and peritoneal tumor burden.[41] Another myeloid subset associated with immunosuppressive regulation, the MDSCs were identified in our study as potential mediators of therapy resistance. MDSCs have been linked to immunosuppression and therapy resistance across different cancer types.[24,25,42]

In line with these flow-cytometry findings, the analyses of serum also provided evidence for systemic immune suppression including higher levels of IL-6, IL-8, IL-10, and VEGF in non-pCR patients. Across tumor types, these have all been related to cancer stage, prognosis, and immune suppression.[43] Important to mention is that the flow cytometry findings in our study seem to be specific for the anti-PD-L1 combination regimen of the PERFECT trial. Determinants of response in PERFECT were mostly immunosuppressive subsets, while in the nCRT-only cohort CD8 T cell abundance and previously identified enrichment for effector memory CD8+ T cells were predictive of pathological response.[7] It thus seems that in anti-PD-L1 non-responders there are specific immunological barriers to mount an effective immune-response both at baseline and throughout the course of treatment.

In the PERFECT patients we established correlations between immunosuppressive pathways from RNA-sequencing data of tumor biopsies and PBMC subsets. At baseline Tregs and circulating monocytes positively correlated with the Wnt/β-Catenin signaling pathway. This pathway can actively regulate immune cell exclusion of the TME by interacting with tumor-associated macrophages and enhance Treg survival through Snail and β-catenin.[28] Other pathways identified by us as positively correlating with intermediate monocytes (hedgehog, myogenesis) and eMDSCs (estrogen, p53) or negatively correlating with cDC2 (pancreas beta cells) have also been linked to immune-cell exclusion and expansion of suppressive immune cells in the TME.[29–32] Additionally, on-treatment we identified overlap in pathways positively correlating with circulating aTregs and a signature for intratumoral Tregs. One of these was angiogenesis, which indeed can be associated with Treg proliferation; in colorectal cancer VEGF-A induced by the tumor can enhance circulating Treg proliferation by binding to VEGFR2.[44] Moreover, anti-VEGF-A (bevacizumab) treatment in colorectal cancer patients reduced Treg proportions in peripheral blood.[44] Another interesting observation was the correlation between the induction of EMT and expansion of aTregs. The relationship between EMT and immune suppression is well established across different tumor types.[17] In esophageal cancer this relationship may in part be due to the release of TGF-β by cancer cells under the influence of chemoradiotherapy and the subsequent conversion of CD4 T-cells into Tregs.[14,15,45] These Tregs are also able to produce TGF-β and thereby even further promote EMT as well as immune suppression.[46] Interestingly in our cohort, the induction of EMT due to nCRT was related not just to a Treg signature in the TME, but also to a change in systemic aTreg rates. The measurement of aTregs by flow cytometry of

peripheral blood could serve as a marker for EMT induction. New therapy combinations could be explored through on-treatment monitoring and stratification based on a positive delta threshold of aTregs or high CD8Ki67/aTreg ratio on-treatment. Turn-around time from sample to result could be available within 1 or 2 days. A potential clinical study design could be based on a PD-1/PD-L1 chemoradiotherapy back-bone and additional escalation in patients with aTreg expansion on-treatment with anti-CTLA4/VEGF-A antibodies to deplete Tregs or selective TGF-β targeting. Important questions do, however, need to be answered in future studies regarding timing, dosing, toxicity, and biomarker validation.

Remarkably, 3 months after surgery, the expression of CD40 on monocytes was predictive for eventual disease recurrence in the PERFECT trial. The CD40 costimulatory receptor can be found on a broad variety of antigen-presenting cells including monocytes.[47] Activation of CD40 on monocytes can lead to the induction of proinflammatory cytokines (IL-1a, IL-1b, TNF-a, IL-6, and IL-12) and chemokines (IL-8, CCL2, CCL3, CCL4, and CCL5).[47] Depending on the context, CD40 on monocytes can be pro-tumorigenic or tumoristatic.[47] Evidence is emerging that CD40 may be involved in the activation status of tumor-associated macrophages and systemic immunosuppression.[47,48] We also found less proliferating CD8+ T-cells in patients with a recurrence indicating there may be systemic barriers suppressing T-cell activity. The outgrowth of subclinical minimal residual disease into apparent metastases could be related to systemic T-cell suppression induced by monocytes and macrophages.[49] In our cohort we found a CD206+ M2-like monocyte subset with potential suppressive capacity (CD163+ and PD-L1+), although we could not establish any functional cytokines which might be involved in such T-cell suppression after M1/M2a stimulation of CD14+ macrophages.[49,50] The latter might be related to the low frequency of CD206+ cells or a different mechanism of action through cell–cell interaction or paracrine signaling. Another aspect relevant in this patient group is the relationship between surgery, inflammation, and the release of immunosuppressive factors.[51] The recruitment of neutrophils and monocytes to the wound bed can reeducate these cell types to become immunosuppressive and pro-tumorigenic.[51] Although it must be noted that surgery-related changes are usually transient, they could nevertheless have created an immune suppressive window.[52,53] In conclusion, after additional validation, the expression of CD40 on monocytes could be a new biomarker for recurrence.

Conclusions

Immuno-monitoring of peripheral blood from rEAC patients by flow cytometry revealed distinct differences in the systemic immune-profile between complete and incomplete responders of the neoadjuvant PERFECT trial. Non-responders were defined by the presence of immunosuppressive subsets such as: Tregs, CD16+ monocytes and eMDSCs as well as elevated levels of immune suppressive cytokines. Pathways activated in the TME and associated with immune-exclusion, including the Wnt/β-Catenin

pathway, positively correlated with these subsets. The abundance of aTregs on-treatment was associated with the angiogenesis pathway and induction of EMT. After surgery monocyte activation (CD40), low rates of CD8+Ki67+ T-cells and the enrichment of CD206+ monocytes were related to early recurrence within 2 years. This study identified systemic immunosuppressive barriers to neoadjuvant immuno-chemoradiotherapy and identified potential targets for future clinical studies.

Acknowledgments

Disclosure statement

MIvBH is consultant for Mylan, Johnson & Johnson, Alesi Surgical, BBraun and Medtronic, and received unrestricted research grants from Stryker. All fees paid to institution. NHM has served as a consultant for MSD, BMS, Astra Zeneca, Servier and Lilly. MFB received research funding from Celgene and Lead Pharma and has acted as a consultant for Servier. HWMvL: Consultant or advisory role: BMS, Daiichy, Dragonfly, Eli Lilly, MSD, Nordic Pharma, Servier. Research funding and/or medication supply: Bayer, BMS, Celgene, Janssen, Incyte, Eli Lilly, MSD, Nordic Pharma, Philips, Roche, Servier. Speaker role: Astellas, Daiichy, Novartis. TDdG reports to be in an advisory role for GE Healthcare, Mendus and LAVA Therapeutics, to have received a research grant from Idera Pharmaceuticals, and to be co-founder and owner of stocks of LAVA Therapeutics, outside of the submitted work. The other authors report no conflict of interest.

Funding

ORCID

Tom van den Ende   http://orcid.org/0000-0003-2830-2310

Authors' contributions

All authors contributed to the design of this study. TvdE, MIvBH, MCCMH, NHM, RvH, SM, NCTvG, MFB, HWMvL, and TDdG were involved in the PERFECT trial including patient care and/or translational research. TvdE, JB, SML, and MH were involved in collecting patient samples and/or isolation of PBMCs. JB, SML, and TDdG developed the immune monitoring panel. TvdE, AE, LMB, JB, MH, and CW performed the data acquisition. TvdE, AE, LMB, MH, HWMvL, and TDdG were involved in data analysis. TvdE was responsible for drafting the manuscript. All authors contributed to the manuscript and read and approved the final manuscript.

Ethics approval and consent to participate

All patients provided written, informed consent for study participation. This study was conducted in accordance with the Declaration of Helsinki and the international standards of good clinical practice.

Consent for publication

We confirm that the manuscript has been read and approved by all named authors.

Availability of data and material

The data that support the findings of this study are available from the corresponding author, [TvdE], upon reasonable request.

References

1. van Hagen P, Hulshof MC, van Lanschot JJ, van Hagen P, van Lanschot JJB, Steyerberg EW, Henegouwen MIVB, Wijnhoven BPL, Richel DJ, Nieuwenhuijzen GAP, et al. Preoperative chemoradiotherapy for esophageal or junctional cancer. N Engl J Med. 2012;366(22):2074–2084. doi:10.1056/NEJMoa1112088.
2. Shapiro J, van Lanschot JJB, Hulshof M, van Hagen P, van Berge Henegouwen MI, Wijnhoven BPL, van Laarhoven HWM, Nieuwenhuijzen GAP, Hospers GAP, Bonenkamp JJ, et al. Neoadjuvant chemoradiotherapy plus surgery versus surgery alone for oesophageal or junctional cancer (CROSS): long-term results of a randomised controlled trial. Lancet Oncol. 2015;16 (9):1090–1098. doi:10.1016/S1470-2045(15)00040-6.
3. Kelly RJ, Ajani JA, Kuzdzal J, Zander T, Van Cutsem E, Piessen G, Mendez G, Feliciano J, Motoyama S, Lièvre A, et al. Adjuvant Nivolumab in resected esophageal or gastroesophageal junction cancer. N Engl J Med. 2021;384(13):1191–1203. doi:10.1056/NEJMoa2032125.
4. van den Ende T, Clercq N, van Berge Henegouwen MI, van den Ende T, van Berge Henegouwen MI, Gisbertz SS, Geijsen ED, Verhoeven RHA, Meijer SL, Schokker S, et al. Neoadjuvant chemoradiotherapy combined with Atezolizumab for Resectable Esophageal Adenocarcinoma: a single arm phase ii feasibility trial (PERFECT). Clin Cancer Res. 2021;27(12):3351–3359. doi:10.1158/1078-0432.CCR-20-4443.
5. Nie R, Chen F, Provencio M, Wang Y, van den Ende T, van Laarhoven HWM, Yuan S, Pless M, Hayoz S, Zhou Z, et al. Predictive value of radiological response, pathological response and relapse-free survival for overall survival in neoadjuvant immunotherapy trials: pooled analysis of 29 clinical trials. Eur J Cancer. 2023;186:211–221. doi:10.1016/j.ejca.2023.03.010.
6. Al-Kaabi A, van der Post RS, van der Werf LR, Wijnhoven BPL, Rosman C, Hulshof MCCM, van Laarhoven HWM, Verhoeven RHA, Siersema PD. Impact of pathological tumor response after CROSS neoadjuvant chemoradiotherapy followed by surgery on long-term outcome of esophageal cancer: a population-based study. Acta Oncol. 2021;60(4):497–504. doi:10.1080/0284186X.2020.1870246.
7. Goedegebuure RSA, Harrasser M, de Klerk LK, van Schooten TS, van Grieken NCT, Eken M, Grifhorst MS, Pocorni N, Jordanova ES, van Berge Henegouwen MI, et al. Pre-treatment tumor-infiltrating T cells influence response to neoadjuvant chemoradiotherapy in esophageal adenocarcinoma. Oncoimmunology. 2021;10(1):1954807. doi:10.1080/2162402X.2021.1954807.
8. Nixon AB, Schalper KA, Jacobs I, Potluri S, Wang I-M, Fleener C. Peripheral immune-based biomarkers in cancer immunotherapy: can we realize their predictive potential? J ImmunoTher Cancer. 2019;7(1):325. doi:10.1186/s40425-019-0799-2.
9. Subrahmanyam PB, Dong Z, Gusenleitner D, Giobbie-Hurder A, Severgnini M, Zhou J, Manos M, Eastman LM, Maecker HT, Hodi FS, et al. Distinct predictive biomarker candidates for response to anti-CTLA-4 and anti-PD-1 immunotherapy in melanoma patients. J ImmunoTher Cancer. 2018;6(1):18. doi:10.1186/s40425-018-0328-8.

10. Kamphorst AO, Pillai RN, Yang S, Nasti TH, Akondy RS, Wieland A, Sica GL, Yu K, Koenig L, Patel NT, et al. Proliferation of PD-1+ CD8 T cells in peripheral blood after PD-1–targeted therapy in lung cancer patients. Proc Natl Acad Sci U S A. 2017;114(19):4993–4998. doi:10.1073/pnas.1705327114.

11. Meyer C, Cagnon L, Costa-Nunes CM, Baumgaertner P, Montandon N, Leyvraz L, Michielin O, Romano E, Speiser DE. Frequencies of circulating MDSC correlate with clinical outcome of melanoma patients treated with ipilimumab. Cancer Immunol Immunother. 2014;63(3):247–257. doi:10.1007/s00262-013-1508-5.

12. Duell J, Dittrich M, Bedke T, Mueller T, Eisele F, Rosenwald A, Rasche L, Hartmann E, Dandekar T, Einsele H, et al. Frequency of regulatory T cells determines the outcome of the T-cell-engaging antibody blinatumomab in patients with B-precursor ALL. Leukemia. 2017;31(10):2181–2190. doi:10.1038/leu.2017.41.

13. Huang Q, Wu X, Wang Z, Chen X, Wang L, Lu Y, Xiong D, Liu Q, Tian Y, Lin H, et al. The primordial differentiation of tumor-specific memory CD8+ T cells as bona fide responders to PD-1/PD-L1 blockade in draining lymph nodes. Cell. 2022;185 (22):4049–4066.e25. doi:10.1016/j.cell.2022.09.020.

14. Wang Y, Li T, Lv J, Xiao L. Irradiated esophageal squamous cell carcinoma cells induced the increase of Treg by TGF-beta. JCO. 2021;39(15_suppl):e16092–e. doi:10.1200/JCO.2021.39.15_suppl. e16092.

15. Steins A, Ebbing EA, Creemers A, Zalm AP, Jibodh RA, Waasdorp C, Meijer SL, Delden OM, Krishnadath KK, Hulshof MCCM, et al. Chemoradiation induces epithelial-to-mesenchymal transition in esophageal adenocarcinoma. Int J Cancer. 2019;145(10):2792–2803. doi:10.1002/ijc.32364.

16. Dongre A, Rashidian M, Reinhardt F. Epithelial-to-mesenchymal transition contributes to immunosuppression in breast carcinomas. Cancer Res. 2017;77(15):3982–3989. doi:10.1158/ 0008-5472.CAN-16-3292.

17. Taki M, Abiko K, Ukita M, Murakami R, Yamanoi K, Yamaguchi K, Hamanishi J, Baba T, Matsumura N, Mandai M, et al. Tumor immune microenvironment during epithelial–mesenchymal transition. Clin Cancer Res. 2021;27 (17):4669–4679. doi:10.1158/1078-0432.CCR-20-4459.

18. Scheffer HJ, Stam AGM, Geboers B, Vroomen LGPH, Ruarus A, de Bruijn B, van den Tol MP, Kazemier G, Meijerink MR, de Gruijl TD, et al. Irreversible electroporation of locally advanced pancreatic cancer transiently alleviates immune suppression and creates a window for antitumor T cell activation. Oncoimmunology. 2019;8(11):1652532. doi:10.1080/2162402X.2019.1652532.

19. Liberzon A, Birger C, Thorvaldsdottir H, Ghandi M, Mesirov J, Tamayo P. The Molecular Signatures Database (MSigDB) hallmark gene set collection. Cell Syst. 2015;1(6):417–425. doi:10.1016/j.cels. 2015.12.004.

20. Vasaikar SV, Deshmukh AP, den Hollander P, Addanki S, Kuburich NA, Kudaravalli S, Joseph R, Chang JT, Soundararajan R, Mani SA, et al. Emtome: a resource for pan-cancer analysis of epithelial-mesenchymal transition genes and signatures. Br J Cancer. 2021;124(1):259–269. doi:10.1038/ s41416-020-01178-9.

21. Gibbons DL, Creighton CJ. Pan-cancer survey of epithelial-mesenchymal transition markers across the cancer genome atlas. Dev Dyn. 2018;247(3):555–564. doi:10.1002/dvdy.24485.

22. De Simone M, Arrigoni A, Rossetti G, Gruarin P, Ranzani V, Politano C, Bonnal RP, Provasi E, Sarnicola M, Panzeri I, et al. Transcriptional landscape of human tissue lymphocytes unveils uniqueness of tumor-infiltrating T regulatory cells. Immunity. 2016;45(5):1135–1147. doi:10.1016/j.immuni.2016.10.021.

23. Budczies J, Klauschen F, Sinn BV, Győrffy B, Schmitt WD, Darb-Esfahani S, Denkert C. Cutoff Finder: a comprehensive and straightforward web application enabling rapid biomarker cutoff optimization. PLoS One. 2012;7(12):e51862. doi:10.1371/journal. pone.0051862.

24. Li K, Shi H, Zhang B, Ou X, Ma Q, Chen Y, Shu P, Li D, Wang Y. Myeloid-derived suppressor cells as immunosuppressive regulators

25. and therapeutic targets in cancer. Sig Transduct Target Ther. 2021;6(1):362. doi:10.1038/s41392-021-00670-9.

25. Liang Y, Wang W, Zhu X, Yu M, Zhou C. Inhibition of myeloid-derived suppressive cell function with all-trans retinoic acid enhanced anti-PD-L1 efficacy in cervical cancer. Sci Rep. 2022;12(1):9619. doi:10.1038/s41598-022-13855-1.

26. Schiott A, Lindstedt M, Johansson-Lindbom B, Roggen E, Borrebaeck CAK. CD27- CD4+ memory T cells define a differentiated memory population at both the functional and transcriptional levels. Immunology. 2004;113(3):363–370. doi:10. 1111/j.1365-2567.2004.01974.x.

27. Pepper M, Jenkins MK. Origins of CD4(+) effector and central memory T cells. Nat Immunol. 2011;12(6):467–471. doi:10.1038/ni.2038.

28. Pai SG, Carneiro BA, Mota JM, Costa R, Leite CA, Barroso-Sousa R, Kaplan JB, Chae YK, Giles FJ. Wnt/beta-catenin pathway: modulating anticancer immune response. J Hematol Oncol. 2017;10 (1):101. doi:10.1186/s13045-017-0471-6.

29. Petty AJ, Li A, Wang X. Hedgehog signaling promotes tumor-associated macrophage polarization to suppress intratumoral CD8+ T cell recruitment. J Clin Invest. 2019;129 (12):5151–5162. doi:10.1172/JCI128644.

30. Ren J, Hou Y, Wang T. Roles of estrogens on myeloid-derived suppressor cells in cancer and autoimmune diseases. Cell Mol Immunol. 2018;15(7):724–726. doi:10.1038/cmi.2017.129.

31. Blagih J, Zani F, Chakravarty P, Hennequart M, Pilley S, Hobor S, Hock AK, Walton JB, Morton JP, Gronroos E, et al. Cancer-specific loss of p53 leads to a modulation of myeloid and T cell responses. Cell Rep. 2020;30(2):481–96 e6. doi:10.1016/j.celrep.2019.12.028.

32. Huang CT, Chang MC, Chen YL. Insulin-like growth factors inhibit dendritic cell-mediated anti-tumor immunity through regulating ERK1/2 phosphorylation and p38 dephosphorylation. Cancer Lett. 2015;359(1):117–126. doi:10.1016/j.canlet.2015.01.007.

33. Andersen LB, Norgaard M, Rasmussen M, Fredsøe J, Borre M, Ulhøi BP, Sørensen KD. Immune cell analyses of the tumor micro-environment in prostate cancer highlight infiltrating regulatory T cells and macrophages as adverse prognostic factors. J Pathol. 2021;255(2):155–165. doi:10.1002/path.5757.

34. Deng L, Zhang H, Luan Y. Accumulation of foxp3+ T regulatory cells in draining lymph nodes correlates with disease progression and immune suppression in colorectal cancer patients. Clin Cancer Res. 2010;16(16):4105–4112. doi:10.1158/1078-0432.CCR-10-1073.

35. Wolf D, Wolf AM, Rumpold H, Fiegl H, Zeimet AG, Muller-Holzner E, Deibl M, Gastl G, Gunsilius E, Marth C, et al. The expression of the regulatory T cell–specific forkhead box transcription factor FoxP3 is associated with poor prognosis in ovarian cancer. Clin Cancer Res. 2005;11(23):8326–8331. doi:10.1158/ 1078-0432.CCR-05-1244.

36. Binnewies M, Mujal AM, Pollack JL, Combes AJ, Hardison EA, Barry KC, Tsui J, Ruhland MK, Kersten K, Abushawish MA, et al. Unleashing type-2 dendritic cells to drive protective antitumor CD4(+) T cell immunity. Cell. 2019;177(3):556–71 e16. doi:10. 1016/j.cell.2019.02.005.

37. Feng AL, Zhu JK, Sun JT, Yang M-X, Neckenig MR, Wang X-W, Shao Q-Q, Song B-F, Yang Q-F, Kong B-H, et al. CD16+ monocytes in breast cancer patients: expanded by monocyte chemoattractant protein-1 and may be useful for early diagnosis. Clin Exp Immunol. 2011;164(1):57–65. doi:10.1111/j.1365-2249.2011.04321.x.

38. Eljaszewicz A, Jankowski M, Gackowska L, Helmin-Basa A, Wiese M, Kubiszewska I, Kaszewski W, Michalkiewicz J, Zegarski W. Clinical immunologyGastric cancer increase the percentage of intermediate (CD14++CD16+) and nonclassical (CD14 +CD16+) monocytes. Cent Eur J Immunol. 2012;4(4):355–361. doi:10.5114/ceji.2012.32725.

39. Subimerb C, Pinlaor S, Lulitanond V, Khuntikeo N, Okada S, McGrath MS, Wongkham S. Circulating CD14(+) CD16(+) monocyte levels predict tissue invasive character of cholangiocarcinoma. Clin Exp Immunol. 2010;161(3):471–479. doi:10.1111/j.1365-2249. 2010.04200.x.

40. Sponaas AM, Moen SH, Liabakk NB, Feyzi E, Holien T, Kvam S, Grøseth LAG, Størdal B, Buene G, Espevik T, et al. The proportion

of CD16 + CD14 dim monocytes increases with tumor cell load in bone marrow of patients with multiple myeloma. Immun Inflamm Dis. 2015;3(2):94–102. doi:10.1002/iid3.53.

41. Prat M, Le Naour A, Coulson K, Lemée F, Leray H, Jacquemin G, Rahabi MC, Lemaitre L, Authier H, Ferron G, et al. Circulating CD14 high CD16 low intermediate blood monocytes as a biomarker of ascites immune status and ovarian cancer progression. J ImmunoTher Cancer. 2020;8(1):e000472. doi:10.1136/jitc-2019-000472.

42. Salvador-Coloma C, Santaballa A, Sanmartin E, Calvo D, García A, Hervás D, Cordón L, Quintas G, Ripoll F, Panadero J, et al. Immunosuppressive profiles in liquid biopsy at diagnosis predict response to neoadjuvant chemotherapy in triple-negative breast cancer. Eur J Cancer. 2020;139:119–134. doi:10.1016/j.ejca.2020.08.020.

43. Lippitz BE. Cytokine patterns in patients with cancer: a systematic review. Lancet Oncol. 2013;14(6):e218–28. doi:10.1016/S1470-2045(12)70582-X.

44. Terme M, Pernot S, Marcheteau E, Sandoval F, Benhamouda N, Colussi O, Dubreuil O, Carpentier AF, Tartour E, Taieb J, et al. VEGFA-VEGFR pathway blockade inhibits tumor-induced regulatory T-cell proliferation in colorectal cancer. Cancer Res. 2013;73 (2):539–549. doi:10.1158/0008-5472.CAN-12-2325.

45. Kondo Y, Suzuki S, Takahara T, Ono S, Goto M, Miyabe S, Sugita Y, Ogawa T, Ito H, Satou A, et al. Improving function of cytotoxic T-lymphocytes by transforming growth factor-β inhibitor in oral squamous cell carcinoma. Cancer Sci. 2021;112 (10):4037–4049. doi:10.1111/cas.15081.

46. Togashi Y, Shitara K, Nishikawa H. Regulatory T cells in cancer immunosuppression - implications for anticancer therapy. Nat Rev Clin Oncol. 2019;16(6):356–371. doi:10.1038/s41571-019-0175-7.

47. Suttles J, Stout RD. Macrophage CD40 signaling: a pivotal regulator of disease protection and pathogenesis. Semin Immunol. 2009;21(5):257–264. doi:10.1016/j.smim.2009.05.011.

48. Huang J, Jochems C, Talaie T, Anderson A, Jales A, Tsang KY, Madan RA, Gulley JL, Schlom J. Elevated serum soluble CD40 ligand in cancer patients may play an immunosuppressive role. Blood. 2012;120(15):3030–3038. doi:10.1182/blood-2012-05-427799.

49. Christofides A, Strauss L, Yeo A, Cao C, Charest A, Boussiotis VA. The complex role of tumor-infiltrating macrophages. Nat Immunol. 2022;23(8):1148–1156. doi:10.1038/s41590-022-01267-2.

50. Kong X, Zhu M, Wang Z, Xu Z, Shao J. Characteristics and clinical significance of CD163+/CD206+M2 mono-macrophage in the bladder cancer microenvironment. Turk J Biol. 2021;45 (5):624–632. doi:10.3906/biy-2104-17.

51. Tang F, Tie Y, Tu C, Wei X. Surgical trauma-induced immunosuppression in cancer: Recent advances and the potential therapies. Clin Transl Med. 2020;10(1):199–223. doi:10.1002/ctm2.24.

52. Tan JT, Zhong JH, Yang Y, Mao N-Q, Liu D-S, Huang D-M, Zhao Y-X, Zuo C-T. Comparison of postoperative immune function in patients with thoracic esophageal cancer after video-assisted thoracoscopic surgery or conventional open esophagectomy. Int J Surg. 2016;30:155–160. doi:10.1016/j.ijsu.2016.04.052.

53. Donlon NE, Davern M, Sheppard AD, O'Connell F, Dunne MR, Hayes C, Mylod E, Ramjit S, Temperley H, Mac Lean M, et al. The impact of esophageal oncological surgery on perioperative immune function; implications for adjuvant immune checkpoint inhibition. Front Immunol. 2022;13:823225. doi:10.3389/fimmu.2022.823225.